An Optimization-based Approach to Time Critical Cooperative Surveillance and Coverage with Unmanned Aerial Vehicles

Ali Ahmadzadeh, James Keller, George J. Pappas, Ali Jadbabaie and Vijay Kumar

I. INTRODUCTION

The use of autonomous air vehicles equipped with cameras for surveillance is a natural but challenging application of robotic technology. Unlike ground robots, aerial platforms have many more operating constraints and their dynamic response typically dictates the nature of their role in such an application. While rotary-winged platforms enable more diverse maneuver options than their fixed-wing counterparts, maneuverability along a three-dimensional flight path imposes significant constraints. There is a class small, electrically powered fixed-wing aerial vehicle that feature body fixed cameras to provide a low-overhead platform with which to conduct surveillance operations. Their advantages are that they are portable, quiet, difficult to spot when aloft, inexpensive to acquire and operate, feature rugged airframes and are as safe as flight vehicles can be as their mass is less than 10kg. Their primary disadvantage in this application is that their flight path and sensor line of sight are highly coupled. We would like to develop a path planning capability to enable this class of vehicles to perform missions arguably outside of their design envelope. The benefits would be a low-cost, portable solution capable of being transported by ground personnel on foot. The system can, therefore, be considered to be mobile. The constraints imposed by selection of this type of air vehicle are summarized in "Table I".

These vehicles have inner loop controllers that provide the requisite stability and control for the navigation autopilots they use so that waypoint navigation using GPS is reliable spatially but temporal performance is affected by ambient winds. Excessive maneuvering can degrade the precision of flight path control. Turns are always coordinated because of the constraint on sideslip. The coupling between flight path and camera for forward looking camera is illustrated in the "Fig.1" where the motion of the camera frame at half-second intervals is shown as the flight path is varied from straight to turning flight over a 12 second period for the vehicle at the highest tier. The vehicle position, camera line-of-sight vector intersection with the ground-plane (center of image), and the camera frame edges on the ground-plane are shown. Aircraft roll dynamics impose a 0.5 sec time constant on roll rate commands and the vehicle turns in response to its bank angle. The "Fig.1" also depicts how vehicle motion is amplified at the camera line-of-sight vector and how the shape of the camera frame on the ground-plane is distorted during turning flight.

This work was supported by the DARPA/AFRL HURT program under contract number FA8650-04-C-7142.

Authors are with GRASP Laboratory, University of Pennsylvania, Philadelphia, PA 19104,USA
{aliahmad,jfkeller, pappasg, jadbabai, kumar}@grasp.cis.upenn.edu

TABLE I

THE CONSTRAINTS OF SMALL, ELECTRICALLY POWERED FIXED-WING AERIAL VEHICLE THAT FEATURE BODY FIXED CAMERAS

Speed (airspeed)	Fixed in 10-20 m/s range
Minimum Turning Radius	On order of 40 to 150m (normal load factor $\leq$ 1.05g in level flight)
Flight Characteristics	Constant airspeed sideslip Control
Degrees of Freedom	2 to 3
Dynamic Response	1 to 2 sec to transition to turning flight
Camera Geometry	Field of View: 20-45 deg, fixed line of sight(forward, to left, or right)

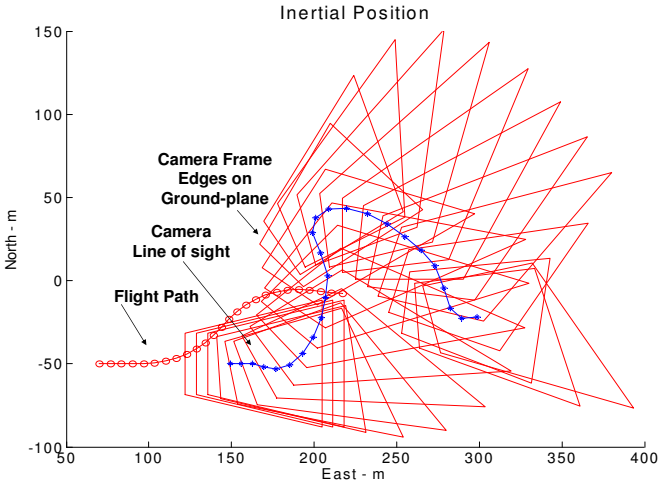

Fig. 1. Front Camera field-of-view on ground plane Camera Parameters: field-of-view 30o, lookdown 30o from horizon, 4x3 frame Aircraft Parameters: airspeed: 15 m/s, altitude: 75m

II. PROBLEM DEFINITION AND FORMULATION

A. Problem Definition

The general problem of interest can be described as follows:

- Given a convex and bounded region $\Omega \subset \Re^2$ and N heterogenous UAVs $\{u_1, u_2, \ldots, u_N\}$, each equipped with a mounted camera and given refresh time τ.
- Find feasible trajectories $\gamma_i(t),\ i = 1,...,N$ for UAVs $u_i,\ i = 1,...,N$ in order to get maximum coverage of the region Ω in each time intervals $[n\tau,(n+1)\tau],\ n = 0,1,...$

We assume that all UAVs fly with fixed and distinct altitudes. The UAVs are modeled as nonholonomic vehicles constrained to move at constant speed v_i $i = 1 \ldots N$ along a path with bounded curvature. A planar trajectory $\gamma_i(t)$ is called flyable by vehicle u_i if it is class C^2 and the absolute value of the signed curvature of the trajectory is always less than $1/\rho_i$ where ρ_i is the minimum radius of a flyable circle by UAV u_i. Since the trajectory $\gamma_i(t)$ of UAV u_i is a planar curve with constant speed v_i, signed curvature function $\kappa_i(t)$ and initial conditions $\gamma_i(t_0)$ and $\theta_i(t_0)$ are sufficient to fully specify trajectory $\gamma_i(t)$ as described in the following theorem.

Theorem 1: Let $\kappa : [t_0, t_0+\tau] \rightarrow [-1/\rho, 1/\rho]$ be a piecewise continuous function with given initial conditions $\gamma(t_0) = (x(t_0), y(t_0))$ and $\theta(t_0)$. Then the parameterized planar trajectory $\gamma : [t_0, t_0+\tau] \rightarrow \Re^2$ can be written as:

$$\gamma(t) = (x(t), y(t)) \tag{1}$$

where

$$x(t) = v \int_{t_0}^{t} \cos(\theta(\zeta)) d\zeta + x(t_0) \tag{2}$$

$$y(t) = v \int_{t_0}^{t} \sin(\theta(\zeta)) d\zeta + y(t_0) \tag{3}$$

and

$$\theta(\zeta) = \int_{t_0}^{\zeta} \kappa(\xi) d\xi + \theta(t_0) \tag{4}$$

Also $\gamma(t)$ is a class C^2 and flyable trajectory for a UAV with constant speed v and initial conditions $\gamma(t_0)$ and $\theta(t_0)$ with maximum turning radius ρ.

This theorem enable us to change the search space from flyable planar trajectories $\gamma_i(t)$ $i = 1, .., N$ to bounded scalar functions $\kappa_i(t)$ $i = 1, .., N$.

Therefore we can restate our objective as generating curvature functions $\{\kappa_i(t) \mid |\kappa_i(t)| \leq 1/\rho_i,\ i = 1, 2, \cdots, N\}$ for all UAVs in order to get maximum coverage for all of the length τ time intervals $[n\tau, (n+1)\tau]$, $n = 0, 1, \ldots$

B. Modeling Camera's Field of View

Each UAV is equipped with either left or front looking camera, left camera mounted on the left wing and front camera mounted in front of the vehicle, both looking at ground with a fixed angle. Since UAVs have to bank to turn, consequently the lookdown angles of the camera change when UAVs turn. As it has been illustrated in "Fig.2" and "Fig.3", the field of view of front camera expands when vehicle turns(left or right) and the field of view of left camera shrinks when vehicle turns left and when vehicle turns right the camera faces horizon and doesn't see anything.

The field of view of each camera(left or front) at any time is a function of position, the orientation and bank angle of the vehicle. Moreover for a given vehicle u_i and a fixed bank angle, the field of view for different positions and orientations differ by a rigid motion.

Assume that $\theta_i(t)$ is the orientation of the vehicle u_i longitudinal axis with respect to the $y = 0$ axis. Also let the bank angle of the vehicle at time t be $\phi_i(t)$. The bank angle

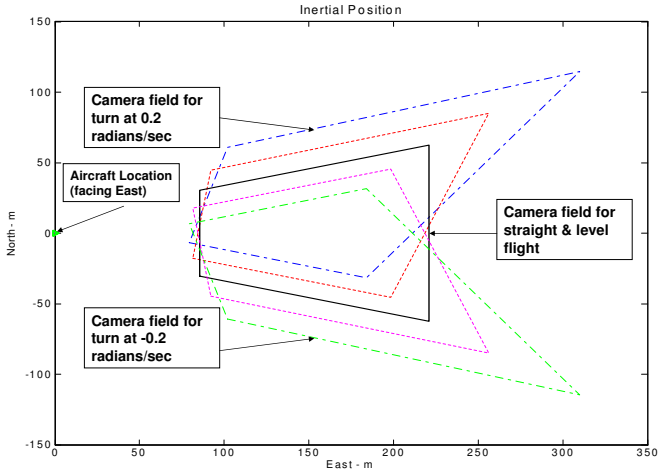

Fig. 2. Front Camera field-of-view on ground plane for turn rates of +0.2 radians/sec in increments of 0.1 radians/sec Camera Parameters: field-of-view 30o, lookdown 30o from horizon, 4x3 frame Aircraft Parameters: airspeed: 15 m/s, altitude: 75m

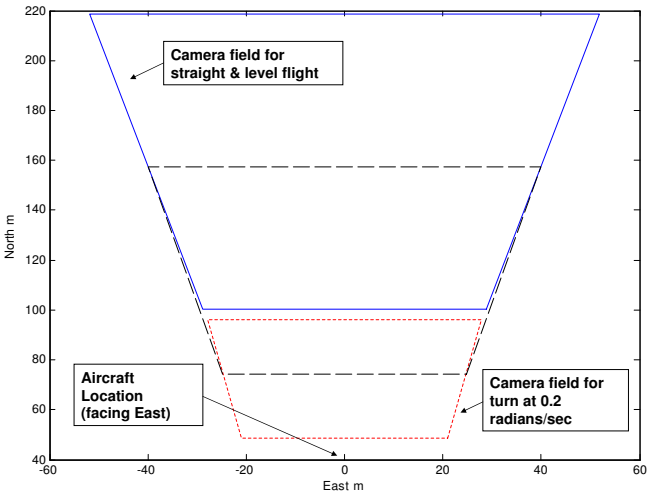

Fig. 3. Left Camera field-of-view on ground plane for turn rates of +0.2 radians/sec in increments of 0.1 radians/sec Camera Parameters: field-of-view 35o, lookdown 30o from horizon, 4x3 frame Aircraft Parameters: airspeed: 17 m/s, altitude: 50m

$\phi_i(t)$ is an explicit function of the curvature of the path $\gamma_i(t)$ and the speed of vehicle at time t and is given as follows:

$$\phi_i(t) = \arctan(v_i^2 \kappa_i(t)/g) \tag{5}$$

Where g is the gravity acceleration.

The orientation of each vehicle $\theta_i(t)$ can be written as:

$$\theta_i(t) = \arctan(y_i(t)/x_i(t)) \tag{6}$$

Given any time instant t_0, the values of $\gamma_i(t_0)$, $\gamma_i'(t_0)$ and $\kappa_i(t_0)$ uniquely specify the field of view at time t_0. Based on this we define the state of configuration of the N-vehicle system as follows.

Definition 1 (state of the system): The state of N-vehicle system $\{u_1, u_2, ..., u_n\}$ with given trajectories $\{\gamma_1, ..., \gamma_N\}$ at

any time t is defined by a $N \times 5$ matrix as:

$$s(t) = \begin{pmatrix} \gamma_1(t) & \gamma_1'(t) & \kappa_1(t) \\ \vdots & \vdots & \vdots \\ \gamma_N(t) & \gamma_N'(t) & \kappa_N(t) \end{pmatrix} = \begin{pmatrix} s_1(t) \\ \vdots \\ s_N(t) \end{pmatrix} \quad (7)$$

As illustrated in Figures 2 and 3, the field of view for any bank angle is a bounded polyhedral set. Let field of view of vehicle u_i with trajectory $\gamma_i(t)$ at time t_0 is given by $\psi_i(s_i(t_0)) \subset \Re^2$. Since $\psi_i(s_i(t_0))$ is a polyhedron, there exist matrices $A(s_i(t_0))$ and $b(s_i(t_0))$ such that:

$$\psi_i(s_i(t_0)) = \{p \in \Re^2 \mid A(s_i(t_0))p \leq b(s_i(t_0))\} \quad (8)$$

We assume that matrices $A(s_i(t_0))$ and $b(s_i(t_0))$ are given for the configurations, where vehicle u_i is located at the origin with orientation $\theta_i(t_0) = 0$ and for all admissible curvatures. For the configuration, where u_i located at $\gamma(t)$ with orientation $\theta_i(t)$ we have:

$$A(s_i(t)) = A(s_i(t_0))Q(-\theta_i(t)) \quad (9)$$

$$b(s_i(t)) = b(s_i(t_0)) - A(s_i(t))\gamma(t) \quad (10)$$

Where the curvature of $s_i(t_0)$ is equal to curvature of $s_i(t)$ and Q is a rotation matrix.

Definition 2 (Coverage map Ψ): At any time t coverage map is mapping from the configuration space to the set Ω as follows:

$$\Psi(s(t)) = \bigcup_{i=1}^{N} \psi_i(s_i(t)) \bigcap \Omega \quad (11)$$

Note that $\Psi(s(t))$ is actually a snapshot of the coverage of Ω at time t.

For a given time interval $[t_0, t_0+\tau]$ and initial state $s(t_0)$ we can state the coverage problem as follow:

$$\max_{\kappa_i(t)} \; area(\bigcup_{i=1\ldots N} \bigcup_{t} \Psi(s(t))) \quad t \in [t_0, t_0+\tau] \quad (12)$$

Note that in (14) the union is over uncountable set $[t_0, t_0+\tau]$ and the union set is not necessary a convex set. Also the Optimization is just in one length τ time period.

C. Discretization of the Space, Curvature and Time

In the following we try to solve (14) using discretization in the set $\Omega \in \Re^2$, curvature functions κ_i and finally time.

1) Discretization of Ω: We partition the search space Ω into regions, using circles with radius r. The tessellation of the field to be observed is based on the geometry of the least capable camera and also the required resolution.

Let $B_r(p)$ represent the ball of radius r and center p as

$$B_r(p) = \{q \in \Re^2 \mid \|p-q\| \leq r\} \quad (13)$$

The collection $\mathscr{C} = \{B_r(p_1), \ldots, B_r(p_n)\}$ is said to cover Ω, or to be a covering of Ω if $\Omega \subseteq \bigcup_{i=1}^{n} B_r(p_i)$.
Given a covering $\mathscr{C}$, the discretized Ω or Ω^d is defined as the following set:

$$\Omega^d = \{B_r(p) \in \mathscr{C} \mid B_r(p) \bigcap \Omega \neq \emptyset\} \quad (14)$$

Similarly we define discretized field of view $\psi_i^d(s_i(t))$ as follows:

$$\psi_i^d(s_i(t)) = \{B_r(p) \in \Omega_d \mid B_r(p) \subseteq \psi_i(s_i(t))\} \quad (15)$$

The following theorem offers an effective and computationally cheap way for computing $\psi_i^d(s_i(t))$.

Theorem 2: Consider $\psi_i(s_i(t))$ as

$$\psi_i(s_i(t)) = \{q \in \Re^2 \mid A_i(s_i(t))q \leq b_i(s_i(t))\} \quad (16)$$

sufficient condition for $B_r(p) \in \psi_i^d(s_i(t))$ is that

$$A_i(s_i(t))p \leq b_i(s_i(t)) - r\varepsilon\mathbf{1} \quad (17)$$

where $\mathbf{1}$ is a vector of ones and:

$$\varepsilon = \|A_i(s_i(t))\|_\infty = \max_j(|a_{j1}| + |a_{j2}|) \quad (18)$$

we also define discretized coverage map $\Psi^d(t)$ as :

$$\Psi^d(s(t)) = \bigcup_{i=1}^{N} \psi_i^d(s_i(t)) \quad (19)$$

2) Discretization of curvature κ_i: Since the range of the function $\kappa_i : [t_0, t_1] \to [-1/\rho_i, 1/\rho_i]$ is bounded, we can fairly approximate function $\kappa_i(t)$ with piecewise constant function $\kappa_i^d(t)$ as:

$$\kappa_i^d : [t_0, t_1] \to \{k_0, k_1, \ldots, k_{2m}\} \quad (20)$$

Where $k_0 = -1/\rho_i < k_1 < \ldots < k_m = 0 < \ldots < k_{2m} = 1/\rho_i$. Also we assume that curvature is constant for a time interval with length δ_1 . In order to make $\kappa_i^d(t)$ a continuous function, we assume that the changes of curvature between two different values k_j to k_l is linear in time and takes δ_2 sec., hence :

$$\kappa_i^d(t) = \frac{(k_l - k_j)}{\delta_2}(t - t_0) + k_j \quad t \in [t_0, t_0+\delta_2] \quad (21)$$

The transition between k_j to k_l is possible iff $|l-j| \leq 1$. Note that δ_1 and δ_2 are actually selected based on dynamic response of the UAVs. Also in the case of constant curvature there is a closed form formula for computing $\gamma(t)$ and $\gamma'(t)$ and $s(t)$. In the case of linear curvature, trapezoid sum approximation method can be applied for computing $\gamma(t)$.

D. Dynamic Programming Formulation

This section presents a dynamic cooperative coverage approach that can be solved as a dynamic programming. To proceed, assume that time is discretized. At any time(stage) t, the decision (control) $\mathscr{U}(t) = (\kappa_1^d(t), \ldots, \kappa_N^d(t))$ is defined to be a vector of constant curvatures for N-vehicle system. Policies are $\pi = \{\mu_0, \mu_1, \ldots, \mu_z\}$, where μ_k maps states $s(t_k)$ into controls $\mathscr{U}(t_j) = \mu_j(s(t_j))$

Bellmans equations for this problem can be written as

$$J_{t_k}(s(t_k)) = \max\{card(\Psi^d(s(t_k)) \bigcap \Omega^d(t_k)) + J_{t_{k+1}}(s(t_{k+1}))\} \quad (22)$$

$$J_{t_n}(s(t_n)) = card(\Psi^c(s(t_n))) \quad \Omega^d(t_n) = \Omega^d \quad (23)$$

Where:

$$\Omega^d(t_k) = \Omega^d(t_{k+1}) - \Psi^d(t_{k+1}) \quad (24)$$

Solving the dynamic programming gives a sequence of optimal curvature vectors for N-vehicle system that defines the trajectories of the vehicles. Note that the horizon in the above dynamic programming problem is n and is finite, but

as stated before the set Ω should be revisited any τ time period. The dynamic programming problem is just for one period. At the end of the time period the configuration of the N-vehicle may be such that, it makes it imposable to recover the area in the next τ period. In order to incorporate the final configuration of the N-vehicle system into the dynamic programming formulation we modify the $J_t(s(t_n))$ as follows:

$$J_t(s(t_n)) = card(\psi^c(t_n) \bigcap \Omega^c) + \Delta(t_n) \tag{25}$$

$$\Delta(t_n) = \sum_i \left(\frac{\omega_i^1}{\|g_i(t_n)\|} - \omega_i^2 \frac{g_i(t_n).g_i^{'}(t_n)}{\|g_i(t_n)\|\|g_i^{'}(t)\|}\right) \tag{26}$$

where $g_i(t)$ is the camera's line of sight.

III. Simulation Results

The cooperative coverage algorithm that is presented in this paper being successfully implemented and tested for surveillance. We are also in the process of generating our own experimental data by the time the full paper is due.

In the simulations we consider a fleet of four vehicles operating at four distinct height-above-ground tiers. To encompass a range of camera parametrization, For the purposes of exhibit, we consider fields of view of 40, 35, 30, and 25 degrees. As webcam type cameras can be used, a 4 x 3 aspect ratio is assumed, with the wide dimension orthogonal to the pitch attitude of the camera. The corresponding camera line-of-sight lookdown angles from level flight are 35, 30, 30 and 25 degrees for altitude tiers of 25, 50, 75 and 100m. In this manner, the widest camera views are placed at the lower tiers to balance the observable areas. Also refresh time τ assumed to be $15sec.$, we considered 5 values for discrete curvature as $\{-1/\rho_i, -1/(2\rho_i), 0, 1/(2\rho_i), 1/\rho_i\}$ also $\delta_1 = 4$ *sec.* and $\delta_2 = 1.5$ *sec.*. The tessellation of the field made by 127 circles with radius $r = 20m$.

These assumptions are made to not incorporate any actual configuration data or limit planner develop to specific models. Figures (5-7) show the generated trajectories for the vehicle for covering civilian neighborhood area bounded by a rectangular region The execution time for generating 300 sec. (solving DP 20 times) trajectories for the UAVs is 7 sec. on a 2 GHz, 768 MB Pentium 4 laptop.

Fig. 4. 300 sec generated trajectory for UAV altitude tiers of 25 with front looking camera

Fig. 5. 300 sec generated trajectory for UAV altitude tiers of 50 with front looking camera

Fig. 6. 300 sec generated trajectory for UAV altitude tiers of 75 with left looking camera

References

[1] E. Arkin, M. Bender, E. Demaine, S. Fekete, J. Mitchell, and S. Sethia, Optimal Covering Tours with Turn Costs, *in Proceedings of the 12th Annual ACM-SIAM Symposium on Discrete Algorithms (SODA 2001)*, Washington, DC, 2001, pp 138-147.

[2] K. Savla, E. Frazzoli, and F. Bullo. On the point-to-point and traveling salesperson problems for Dubins' vehicles. *In Proc. of the American Control Conference*, 2005.

[3] D. P. Bertsekas, *Dynamic Programming and Optimal Control*, Athena Scientific, Belmont, Massachusetts, 2000.

[4] J. Cortes, S. Martinez, T. Karatas, and F. Bullo, Coverage control for mobile sensing networks. *In Proceedings of IEEE International Conference on Robotics and Automation*, 2002, pp. 13271332.

[5] Y. Guo, L. E. Parker, and R. Madhavan, Towards collaborative robots for infrastructure security applications, *in Proceedings of The 2004 International Symposium on Collaborative Technologies and Systems*, San Diego, CA, Jan. 2004, pp. 235240.

Fig. 7. 300 sec generated trajectory for UAV altitude tiers of 100 with front looking camera

[6] A.Zelinsky, R. A. Jarvis, J. C. Byrne, and S. Yuta, Planning paths of complete coverage of an unstructured environments by a mobile robot *in Proceedings of IEEE International Conference on Robotics and Automation*, 1993, pp. 26122619.

[7] R. Kershner, The number of circles covering a set. *Amer. J. Math.*, vol. 61, pp. 665671, 1939.

[8] Do Carmo M.P., *Differential geometry of curvs and surfaces*, Prentice Hall, 1976.

[9] M. Batalin, G. Sukhatme, Coverage, Exploration and Deployment by a Mobile Robot and Communication Network, *In Telecommunication Systems Journal, Special Issue on Wireless Sensor Networks*, Vol. 26, No. 2, pp. 181-196, 2004

[10] E. U. Acar, H. Choset, A. A. Rizzi, P. N. Atkar, and D. Hull, Morse decompositions for coverage tasks, *The Int. J. Robotics Research*, Vol. 21 No. 4, pp. 331344, 2002.

[11] H. Choset, Coverage for robotics–a survey of recent results, *Annals of Mathematics and Artificial Intelligence* Vol. 31 , pp. 113-126, 2001